Supplementary Information (SI) for Nanoscale.
This journal is © The Royal Society of Chemistry 2025

Supporting Information

Stepwise Electrochemical Reconstruction of Bi-Based Anode for Enhanced Aqueous Battery Energy Storage

Jiale Lei, Jinyue Song, Zhaoyang Song, Honggang Fan, Yanpeng Wang, Yusheng Luo, Shuang Liu, Yongcheng Jin and Wei Liu**

School of Materials Science and Engineering, Ocean University of China, Qingdao 266100, People's Republic of China. Email: weiliu@ouc.edu.cn (W. Liu)

Supplementary Equation:

$$D = R^2T^2/2A^2n^4F^4C^2R\sigma^2 \qquad (1)$$

$$Z' = Rs + Rct + \sigma\omega^{-1/2} \qquad (2)$$

Where $\boldsymbol{R}$ (J mol^{-1} K^{-1}), $\boldsymbol{T}$ (K), $\boldsymbol{A}$ (cm^{-2}), $\boldsymbol{n}$, $\boldsymbol{F}$ (C mol^{-1}), $\boldsymbol{C}$ (L mol^{-1}), $\boldsymbol{\sigma}$ and $\boldsymbol{\omega}$ (Hz) are the gas constant, absolute temperature, reaction area of electrode, quantity of transferred electrons, Faraday constant, concentration of electrolyte, Warburg diffusion coefficient, and angular frequency, respectively.

Supplementary Figures:

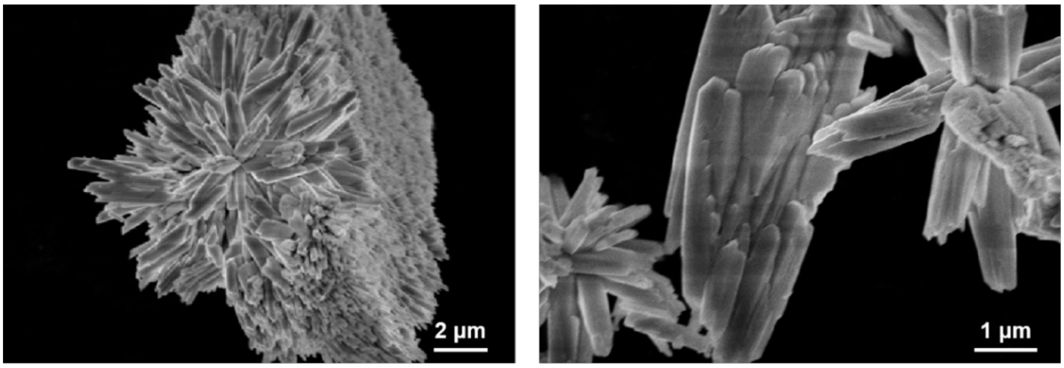

Figure S1. SEM images of α-Bi_2O_3.

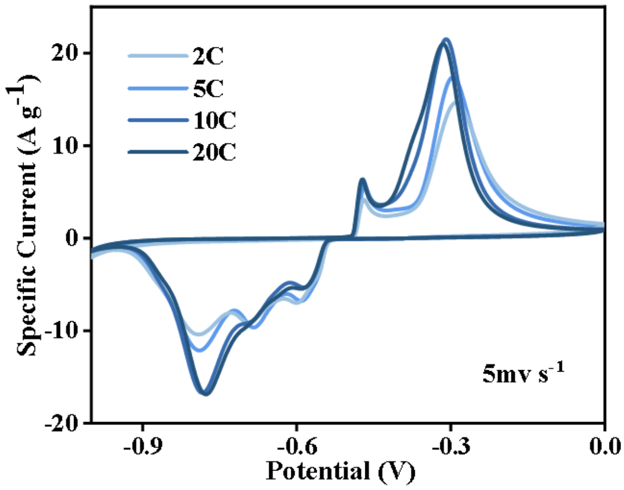

Figure S2. CV curves obtained at varying numbers of electrochemical reconstruction cycles.

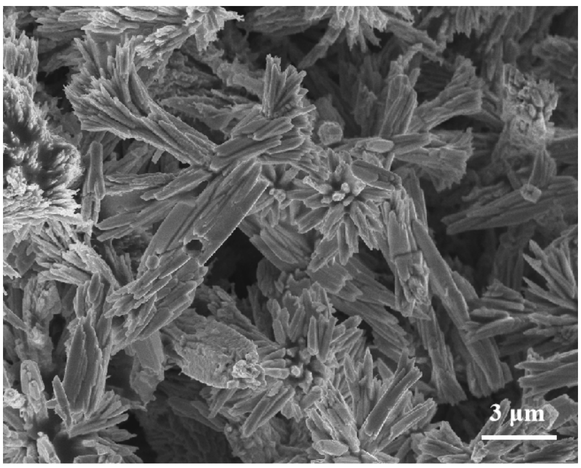

Figure S3. SEM image of electrochemically restructured in the fifth cycle.

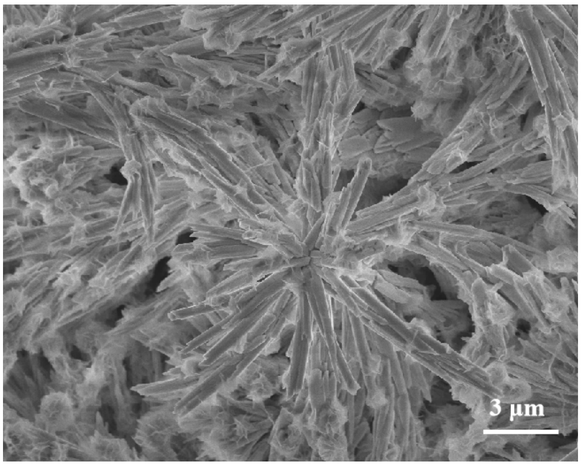

Figure S4. SEM image of BiO_x@BiO/Bi electrochemically restructured in the tenth cycle.

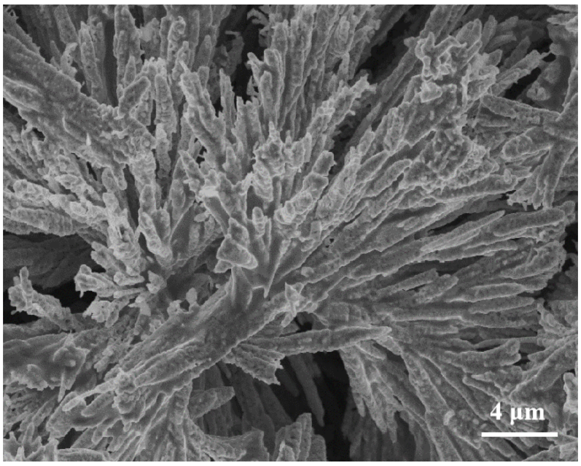

Figure S5. SEM image of BiO_x@BiO/Bi electrochemically restructured in the fifteenth cycle.

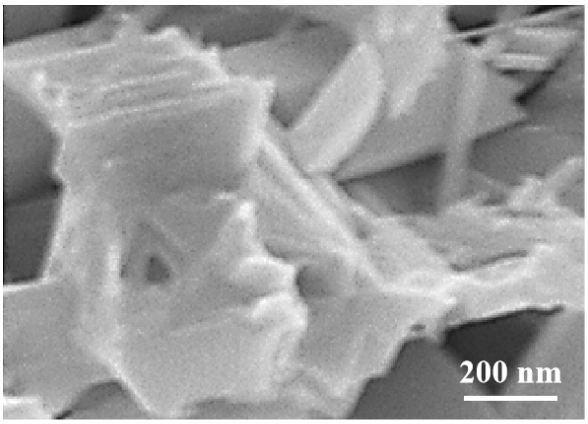

Figure S6. SEM image of the CV activation without α-Bi_2O_3 electrolyte.

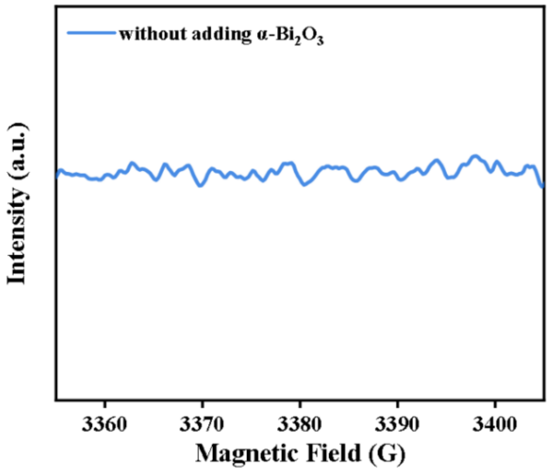

Figure S7. EPR spectra of without adding α-Bi_2O_3 after CV activation.

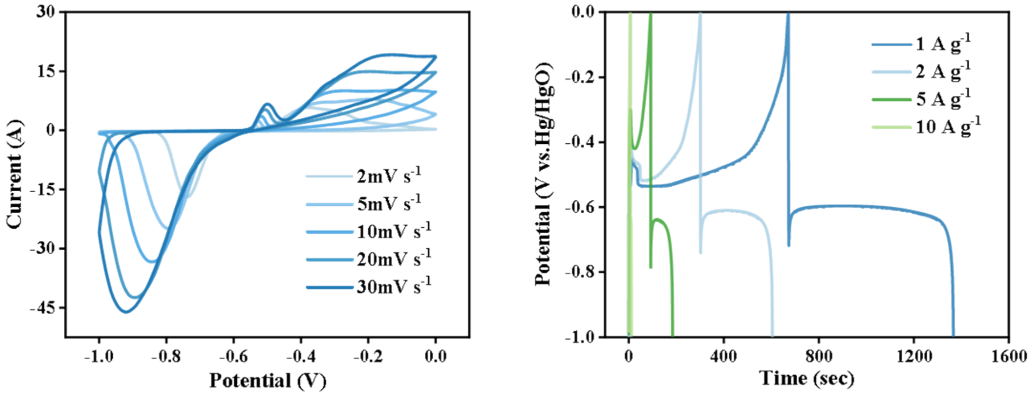

Figure S8. CV and GCD curves of α-Bi_2O_3 electrode.

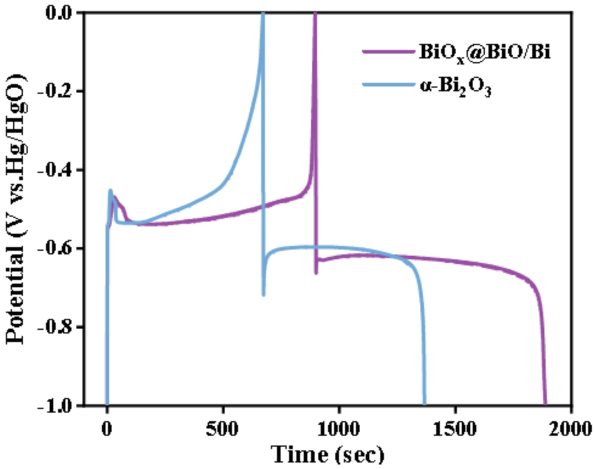

Figure S9. GCD curves of α-Bi_2O_3 and BiO_x@BiO/Bi electrode.

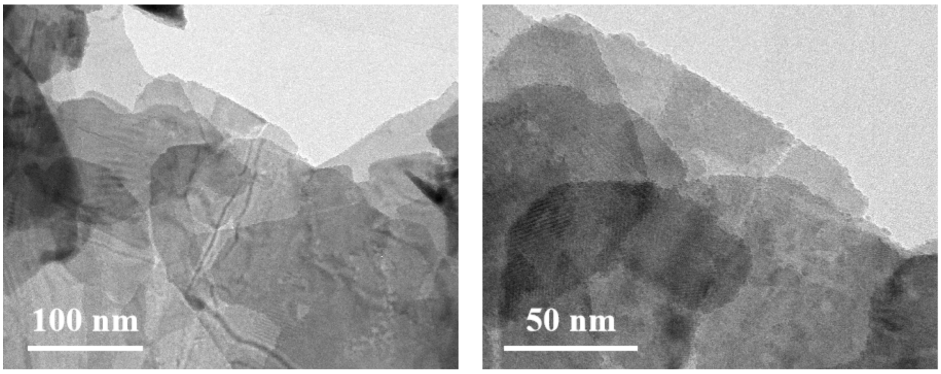

Figure S10. TEM image of BiO_x@BiO/Bi in the charged state.

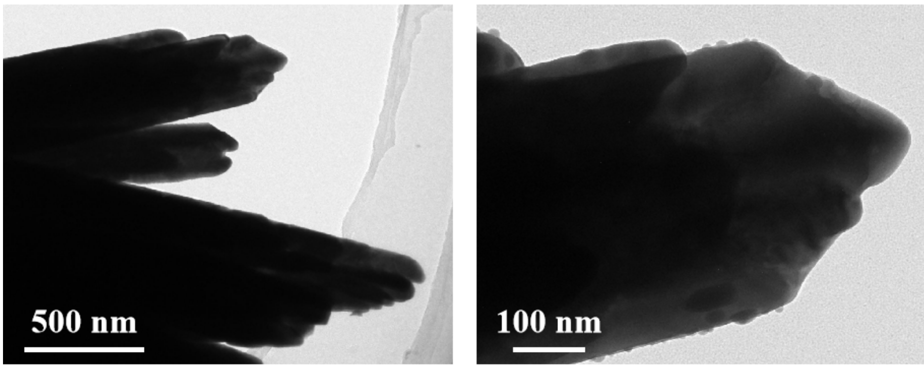

Figure S11. TEM images of BiO_x@BiO/Bi in the discharged state.

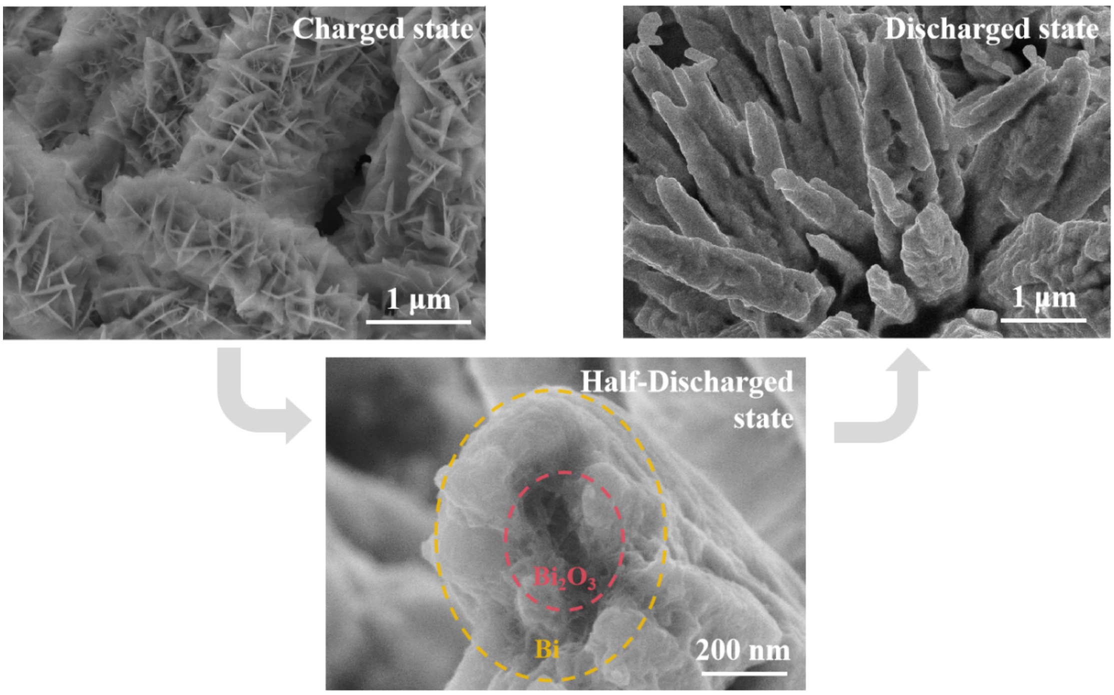

Figure S12. SEM images of BiO_x@BiO/Bi at the discharged state, half-discharged state and charged state after 1000 cycles.

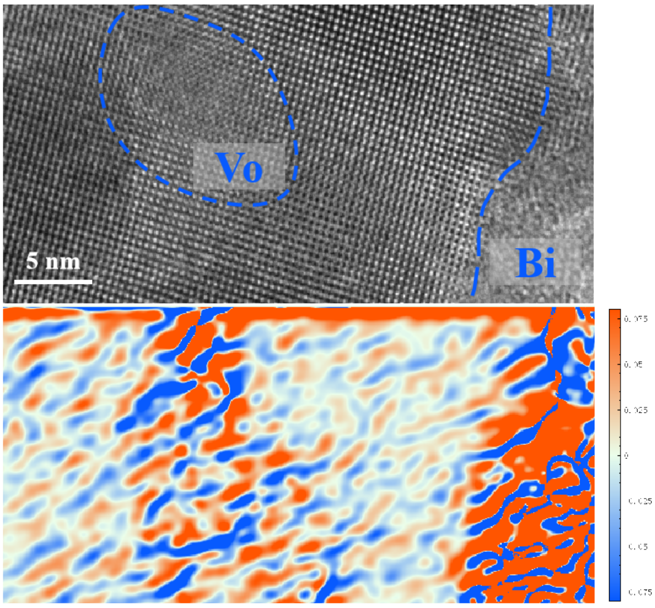

Figure S13. Stress simulation diagram of BiO_x@BiO/Bi (red represents tensile stress, blue represents compressive stress).

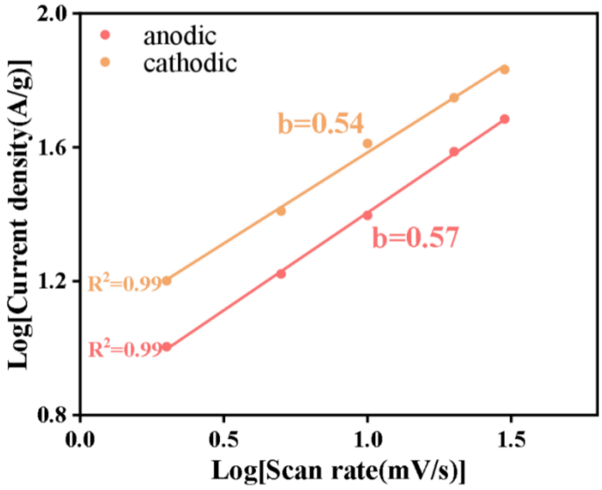

Figure S14. BiO_x@BiO/Bi electrode of the relationship between peak currents and scan rates.

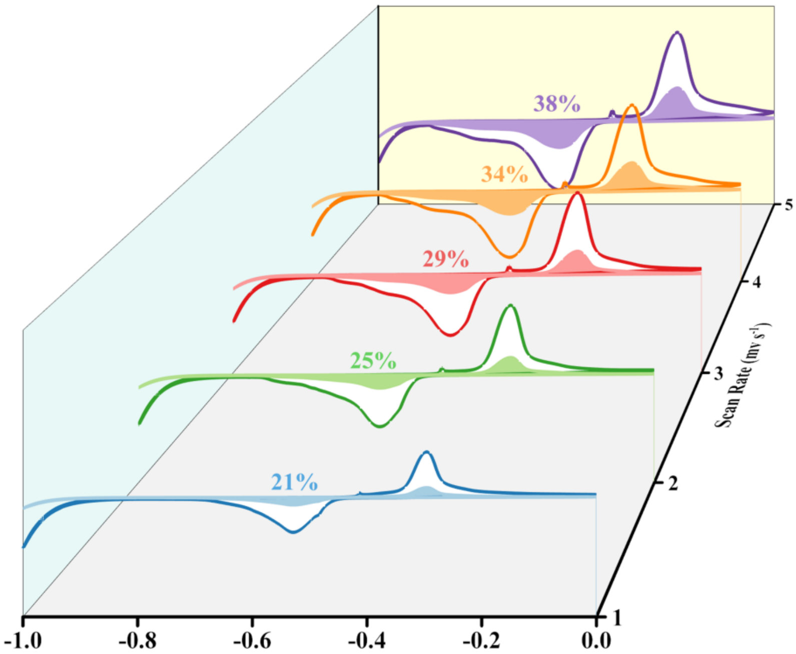

Figure S15. CV curves of the contribution rates of the capacitance and diffusion-controlled capacitance at different scanning rates for BiO_x@BiO/Bi.

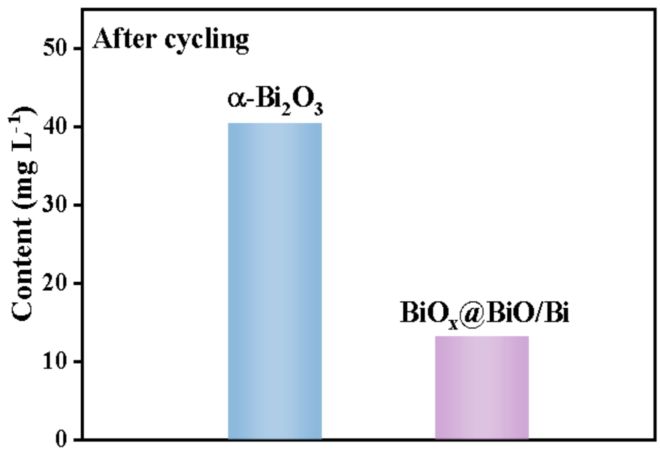

Figure S16. Bi concentration of different sample after 2000 cycles.

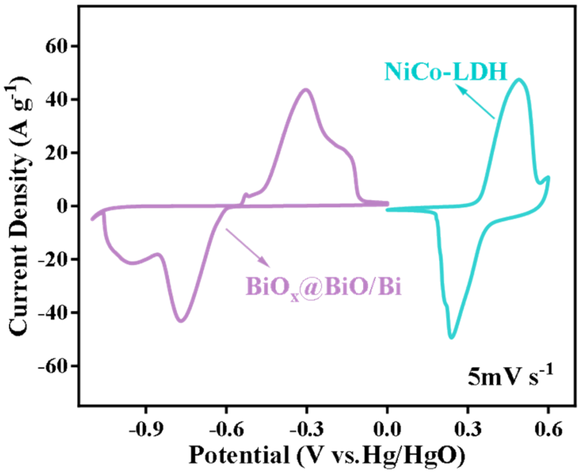

Figure S17. The CV curves of the NiCo-LDH and BiO_x@BiO/Bi electrodes examined at scan rate of 5 mV s^{-1}.

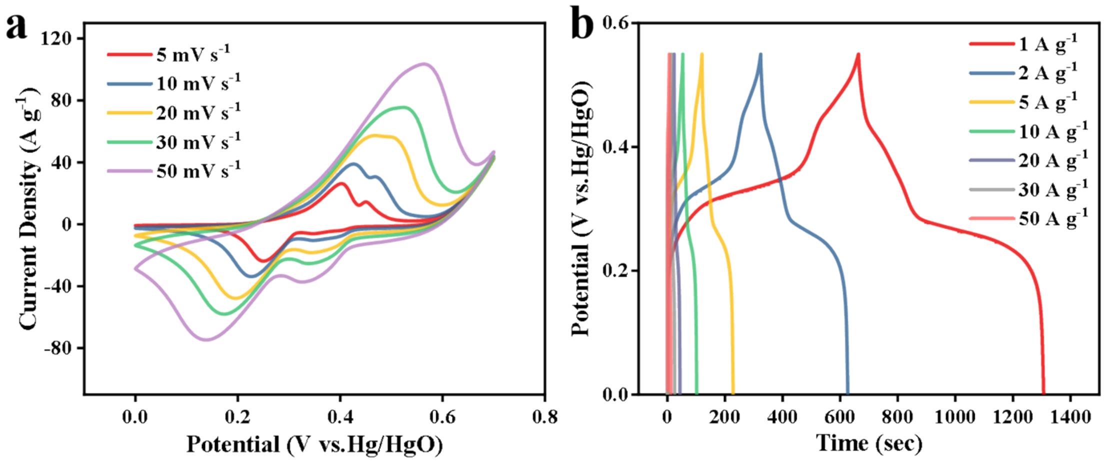

Figure S18. (a) The CV and (b) GCD curves of NiCo-LDH.

Table 1. The specific surface area and pore structure of α-Bi_2O_3 and BiO_x@BiO/Bi.

Sample	S_{BET}[$m^2\ g^{-1}$]	V_{pore}[$cm^3\ g^{-1}$]	D_{aver}[nm]
α-Bi_2O_3	1.9207	0.010176	21.192
BiO_x@BiO/Bi	12.906	0.089317	27.681

S_{BET}: BET surface area

V_{pore}: Total pore volume

D_{aver}: Average pore size

Table 2. The cyele durability of BiO_x@BiO/Bi electrode comparison with the latest reported bismuth-based anodes.

Electrode	Current Density	Cycle Numble	Capacity Retention	Reference
Bi	0.52 A g^{-1}	1700	88.8%	1
Bi_2O_3 rods/RGO	2 A g^{-1}	1000	94%	2
$Bi_2O_2CO_3$/RGO-100	5 A g^{-1}	1000	84.5%	3
Bi-Bi_2O_3/CNT	1 A g^{-1}	1000	72.9%	4
Bi_2Se_3@C	2 A g^{-1}	1500	82.9%	5
Bi_2O_3/porous-RGO	0.5 A g^{-1}	3000	81.1%	6
Bi_2O_3/rGO	5 A g^{-1}	1000	30%	7
Bi/CN_x	1 A g^{-1}	1000	79%	8
BiO_x@BiO/Bi	**2 A g^{-1}** **5 A g^{-1}**	**7000** **3000**	**103.4%** **101.7%**	**This Work**

Reference

1 T. Qin, X. Chu, T. Deng, B. Wang, X. Zhang, T. Dong, Z. Li, X. Fan, X. Ge, Z. Wang, P. Wang, W. Zhang and W. Zheng, *J. Energy Chem.*, 2020, **48**, 21-28.

2 D. Maruthamani, S. Vadivel, M. Kumaravel, B. Saravanakumar, B. Paul, S. S. Dhar, A. Habibi-Yangjeh, A. Manikandan and G. Ramadoss, *J. Colloid Interface Sci.*, 2017, **498**, 449-459.

3 L. Gurusamy, S. Anandan and J. J. Wu, *Electrochim. Acta.*, 2017, **244**, 209-221.

4 H. Wu, J. Guo and D. Yang, *J. Mater. Sci. Technol.*, 2020, **47**, 169-176.

5 H. Qin, Y. Lv, P. Li, M. Xiao, H. Song, Q. Zhang and J. Yang, *New J. Chem.*, 2021, **45**, 21888-21895.

6 L. Gurusamy, S. Anandan, N. Liu and J. J. Wu, *J. Electroanal. Chem.*, 2020, **856**, 113489.

7 S. Liu, Y. Wang and Z. Ma, *Int. J. Electrochem. Sci.*, 2018, **13**, 12256-12265.

8 D. S. Butenko, X. Zhang, I. V. Zatovsky, I. V. Fesych, S. Li, R. Chen, M. Chufarov, O. Symonenko, N. I. Klyui and W. Han, *Dalton Trans.*, 2020, **49**, 12197-12209.